

Computational models of hair cell bundle mechanics: I. Single stereocilium

John Cotton, Wally Grant *

*Department of Engineering Science and Mechanics and School of Biomedical Engineering and Sciences,
Virginia Polytechnic Institute and State University, Mail Code 0219, Blacksburg, VA 24061, USA*

Received 21 April 2003; accepted 21 June 2004
Available online 1 September 2004

Abstract

A distributed parameter model for describing the response of a stereocilium to an applied force is presented. This model is based on elasticity theory, plus the geometry and material properties of the stereocilium. The stereocilia shaft above the taper is not assumed to be perfectly rigid. It is assumed to be deformable and that two separate mechanisms are involved in its deformation: bending and shear. The influence of each mode of deformation is explored in parametric studies. Results show that the magnitude of tip deflection depends on the shear compliance of the stereocilium material, the degree of base taper, and stereocilium height. Furthermore, the deformation profiles observed experimentally will occur only if there are constraints on the geometry and material properties of the stereocilium.

© 2004 Elsevier B.V. All rights reserved.

Keywords: Stereocilia computational model; Stereocilia deformation; Actin shear deformation

1. Introduction

In this paper, we propose a stereocilium model that distributes the stiffness of the stereocilium along the entire height of the structure. This distributed parameter model is based upon the theory of deformable bodies, which is used widely in engineering practice (Beer and Johnson, 2001). Model parameters describe the intrinsic physical properties of the constitutive material and the observable geometry of the stereocilium. The model output describes deformation along the entire shaft as a function of stereocilium height and has an infinite number of degrees of freedom. In the companion papers, we combine two or more of these stereocilia to model the mechanical behavior of both a single line of stereocilia and full three dimensional hair bundles.

Early stereocilium models (e.g., Howard and Ashmore, 1986; Pickles, 1993) lump the resistance to deflection into a single parameter (Fig. 1(a)). This single parameter is analogous to a torsional spring located at the base of a stereocilium modeled as a rigid shaft. In such a model the applied force (or moment) may be divided by the torsional spring stiffness, K , to determine a single deflection value – either linear displacement of the tip, or angular displacement of the stereocilium. This stiffness value, K , is experimentally determined, or selected to match observed deflections for a range of bundle morphologies. The stereocilium itself is considered a rigid shaft that does not deform, so the response can be described by a single parameter (e.g. angular rotation), and the system is said to have a single degree of freedom.

The use of a distributed parameter model results in more accurate deformation descriptions than earlier models (Fig. 1(b)). We will show that this accuracy is insignificant for determining tip deflection of some ciliary geometries; for other geometries, the fuller descrip-

* Corresponding author. Tel.: +1-540-231-4573.
E-mail address: jgrant@vt.edu (W. Grant).

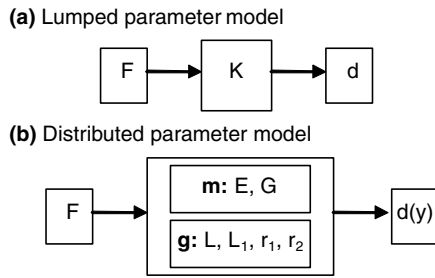


Fig. 1. Comparison of lumped parameter and distributed parameter models. The models convert an applied force, F , to a displacement, d or $d(y)$, where y is the vertical coordinate. Material (m) and geometric (g) properties of the stereocilium shaft determine the response of the distributed parameter model.

tion is essential. The distributed parameter model is also needed to describe deformation along the shaft with the accuracy required for mechanical analyses of whole ciliary bundles. This stereocilium model has been used previously (Cotton, 1998; Cotton and Grant, 2000) and is the basic element of our full bundle models.

Any stereocilium has a high aspect ratio (ratio of height to radius) and a circular cross-section; its base tapers to an insertion point in the sensory epithelium (Fig. 2; Lewis, 1985; Pickles and Corey, 1992). If such a stereocilium is subjected to a point load force perpendicular to its height, applied at the top ($y=L$), basic elasticity theory requires that it experiences both an internal shear force and an internal bending moment (Fig. 3). The magnitude of this shear force is constant over the length of the shaft (Fig. 3(c)), while the moment increases linearly from the top, down the shaft (Fig. 3(d)). Forces applied at different points and distributed force loadings also produce internal shear and bending moments, different from that shown in Fig. 3.

In response to these two internal force loads, the stereocilium deforms (Fig. 4). The shear force induces a shear deformation, while the moment causes bending.

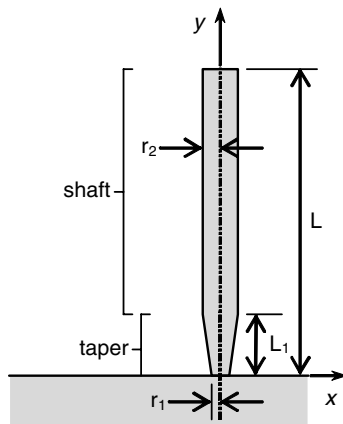


Fig. 2. Geometry of a single stereocilium. The vertical coordinate is y , and the horizontal deflection of the stereocilium when a force is applied is x . Height is L , L_1 is the taper height, r_1 is the base radius and r_2 is the shaft radius.

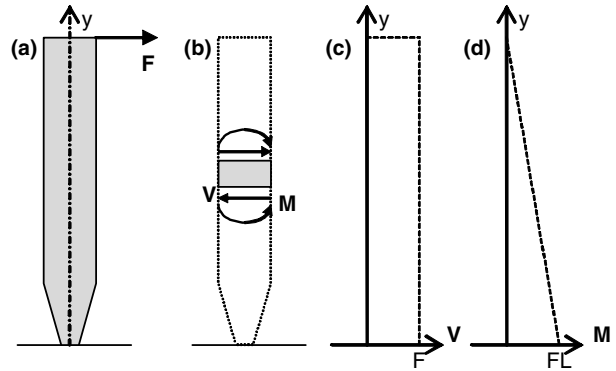


Fig. 3. Under a transverse force load F , such as shown in (a), the stereocilium will undergo internal shear force V and bending moments M , shown on the element in (b). The shear force V , of the point load force is a constant magnitude F , as shown in (c) while the moment M , increases linearly from zero to reach a maximum value at the base equal to FL ($F \times L$), shown in (d).

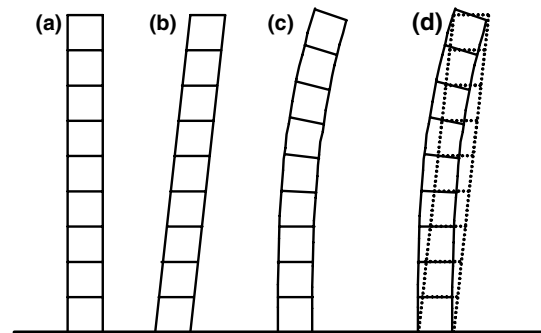


Fig. 4. An untapered stereocilium (a) is used to show the difference between bending and shear deflection. Under shear deformation (b), and under bending (c). The two modes are superposed in (d) with identical tip deflections so the effect on the shaft can be more clearly seen.

Under the point force load shown, shear results in a linear deformation profile (Fig. 4(b)). Deformation due to bending can be described with a third order polynomial as a function of height (Fig. 4(c)). The slope of the cross-section stays parallel to the apical surface of the cell under shear (Fig. 4(b)), but rotates as a second order polynomial of height under bending (Fig. 4(c)).

The resistance to these force loads at each cross-section along the height of the stereocilia is defined by both material and geometric parameters. Materially, the resistance to shear is described by a constant value called the shear modulus, G , while the resistance to bending is described by Young's modulus, E . Geometrically, shear is resisted by the area of the cross-section, while bending is resisted by the area moment of inertia, I . This moment of inertia measures how much material is present at a distance from the centroid of the cross-section, and for a circular cross-section is given by

$$I = \frac{\pi}{4} r^4, \tag{1}$$

where r is the radius of the cross-section. Thus bending is greatest in regions such as the tapered stereocilium base where the radius is small.

For structures with high aspect ratios (height/width) such as stereocilia, bending generally dominates the deformation. This is increasingly true as the aspect ratio increases. However, three factors support that shear also plays a significant role in stereocilium deformation:

(1) A stereocilium is made up of filamentous actin (f-actin) oriented parallel to its long axis (Flock and Chung, 1974; Tilney et al., 1983; Saunders et al., 1985). This internal structure resists the axially oriented tensile and compressive forces seen in bending and confers a higher resistance to bending than to shear in which fibers merely slide past each other (Jones, 1999). Directionally biased structures such as this are said to be transversely isotropic, and they often shear more easily than structures with no directional bias (Jones, 1999). For clarification, an isotropic material has the same deformation properties in all directions, and an anisotropic material has different deformation properties when measured in different directions. In terms of a stereocilia, a transversely isotropic material has different material properties in a direction transverse to the long axis of the stereocilia.

(2) Early finite element models using isotropic stereocilia produced a paradox (Duncan, 1993; Duncan and Grant, 1998). An isotropic material has a shear modulus of approximately one-half to one-third of its Young's modulus (Beer and Johnson, 2001; Jones, 1999). Under the assumption of isotropy, a realistic Young's modulus value of 10^9 N/m² (Gittes et al., 1993) produced bundles much stiffer than observed experimentally. A lower Young's modulus produced realistic values of bundle stiffness, but the lack of bending resistance led to buckling of the bundle, which is not observed experimentally. Realistic deformation shapes and stiffness magnitudes could only be obtained by decoupling bending and shear, which is consistent with the behavior of transversely isotropic structure. As noted above, such structures are relatively susceptible to shear.

(3) Electron microscope images of deformed stereocilia material support the hypothesis that the stereocilium undergoes significant shear (Tilney et al., 1983). In these images, the actin fibers and cross-links between them can be visualized. When the bundle is deflected, the cross-links appear to remain parallel to the apical surface of the hair cell, as shearing would predict (see Fig. 4(b)).

2. Methods

We developed the proposed model in four steps. First, we formulated the problem from first principles of elasticity theory. Second, we non-dimensionalized

the problem to reduce the number of parameters that need to be adjusted. Third, we bracketed these parameters to produce mechanical behavior that matches experimental results on ciliary bundles and the constituent material of the stereocilium. Fourth, when appropriate (e.g., to calculate stereocilium stiffness), we redimensionalized the problem to derive numbers that can be compared with experimental results.

2.1. The stereocilium: description and assumptions

The stereocilium model has two parts (Fig. 2). The *shaft* is assumed to have a circular cross-section and a constant diameter; circular cross-sections have been observed experimentally, and the assumption of constant shaft diameter is accurate for most stereocilia (Lindeman, 1973; Lim, 1977; Lewis, 1985; Duncan, 1999). The stereocilium tapers at its base to an insertion point; we assume this *taper* to be linear. Geometrically, each stereocilium can be described by its overall height, L , the height of its tapered base, L_1 , the radius of its shaft, r_2 , and the radius of its insertion point, r_1 (Fig. 2).

We assume that the stereocilium is firmly held at its base. We base this on (1) experimental observations (Tilney et al., 1983) of rootlet fibers that extend from the insertion point deep into the cuticular plate, and (2) earlier models, which showed that a rigid base and a realistically deformable base produce identical results (Duncan and Grant, 1998).

2.2. Tip deflection

We model two mechanisms of tip deflection: bending and shear. Linear superposition is valid for the small deflections that a stereocilium undergoes. Thus, the total tip deflection of a stereocilium, x , is the sum of bending deformation x_B and shear deformation x_S (Fig. 4(d)),

$$x = x_B + x_S. \quad (2)$$

Using energy methods and Castigliano's theorem (Beer and Johnson, 2001), the deflection from bending can be derived. This is done by computing the total strain energy is one component from bending and the other from shear, then applying the Castigliano's theorem one can get deflection directly. The bending deflection is

$$x_B = \int_0^L \left[\frac{-M(y)}{EI(y)} \right] (L - y) dy, \quad (3)$$

and the deformation from shear is

$$x_S = \int_0^L \frac{kV(y)}{GA(y)} dy, \quad (4)$$

where M =moment, V =shear, I =the area moment of inertia, and A =cross-sectional area, and all are functions of stereocilium height, y (as indicated by (y)) (see

Duncan, 1993 for the derivation); E = Young’s modulus, and G = shear modulus, both moduli are constant in this formulation; and k = a shear correction factor, which is 4/3 for a circular cross-section (Boresi, 1993).

Normalizing the variables and parameters to make them dimensionless (non-dimensionalization), allows reduction of the number of parameters and provides insight into relevant quantities defining deformation. Two non-dimensional variables, denoted by overbars: height \bar{y} and displacement \bar{x} , and four non-dimensional parameters: stereocilium height \bar{L} , taper radius, \bar{r}_1 , shaft radius \bar{r}_2 , and shear modulus, \bar{G} are defined in Table 1. These non-dimensional variables and parameters are introduced into Eqs. (3) and (4), and upon integration for the specific point loaded force case depicted in Fig. 3(a), the tip deflection of the stereocilium is

$$\bar{x} = \bar{x}_B + \bar{x}_S, \tag{5}$$

where

$$\bar{x}_B = 3 \int_0^1 \left\{ \frac{(\bar{L} - \bar{y})^2}{\bar{r}(\bar{y})^4} \right\} d\bar{y} + (\bar{L}^3 - 3\bar{L}^2 + 3\bar{L} - 1), \tag{6}$$

and

Table 1
Non-dimensional variables and parameters

Variable	Non-dimensional variable
Height – y	$\bar{y} = \frac{y}{L_1}$
Displacement – x	$\bar{x} = \left(\frac{3\pi}{4}\right)\left(\frac{Er_2^3}{H^3}\right)x$
Parameter name	Non-dimensional definition
Stereocilium height	$\bar{L} = \frac{L}{L_1}$
Taper radius	$\bar{r}_1 = \frac{r_1}{r_2}$
Shaft radius	$\bar{r}_2 = \frac{r_2}{L_1}$
Shear modulus	$\bar{G} = \frac{G}{kE}$
Shear compliance	$Sh = \frac{3}{4} \left(\frac{\bar{r}_2^3}{\bar{G}}\right)$

Table 2
Values used for parametric studies

	Maximum value	Minimum value	References
<i>Dimensional parameters</i>			
Base radius, r_1	0.25 μm	0.01 μm	Measured from TEM and Howard et al. (1988)
Body radius, r_2	0.25 μm	0.1 μm	Measured from TEM
Taper height, L_1	1.0 μm	No taper	Measured from TEM
Total height, L	100 μm	2.0 μm	Measured from LM and SME
Young’s modulus, E	$3 \times 10^9 \text{ N/m}^2$		Gittes et al. (1993)
Shear modulus, G	$2 \times 10^9 \text{ N/m}^2$	$4 \times 10^4 \text{ N/m}^2$	Cotton and Grant (2000)
Shear correction factor, k	1.33		Boresi (1993)
<i>Non-dimensional parameters</i>			
$\bar{L} = L/L_1$	100	2	
$\bar{r} = r_1/r_2$	1 (no taper)	0.1	
$Sh = (3/4)(\bar{r}_2)^2/\bar{G}$	$\sim 10^3$	$\sim 10^{-2}$	
$\bar{G} = G/(kE)$	$\sim 10^0$	$\sim 10^{-5}$	
$\bar{r}_2 = r_2/L_1$	0.25	0.1	

Values of non-dimensional shear modulus and shear compliance were approximated by their order of magnitude ($\sim 10^x$).

$$\bar{x}_S = \frac{3}{4} \left(\frac{\bar{r}_2^2}{\bar{G}}\right) \left[\frac{1}{\bar{r}_1} + \bar{L} - 1\right]. \tag{7}$$

The function $\bar{r}(\bar{y})$ is the radius in the stereocilium, defined in the taper by the function,

$$\bar{r}(\bar{y}) = \bar{r}_1 + (1 - \bar{r}_1)\bar{y} \quad 0 \leq \bar{y} \leq 1. \tag{8}$$

The two non-dimensional parameters \bar{G} and \bar{r}_2 may be combined into a single parameter (see Eq. (7)). This value represents the shear compliance and will be denoted by Sh such that

$$Sh = \frac{3}{4} \left(\frac{\bar{r}_2^2}{\bar{G}}\right). \tag{9}$$

The total non-dimensional tip deflection of the above model reduces to a function of three non-dimensional variables: the non-dimensional height \bar{L} , the non-dimensional taper radius \bar{r}_1 , and the shear compliance Sh. Eq. (6) was numerically integrated using Simpson’s method to obtain deflection.

Parametric studies of non-dimensional tip deflections were computed with variations in stereocilium height, taper, and shear compliance. Ranges for each non-dimensional parameter and for their underlying dimensional parameters are presented in Table 2. Table 3 presents the effects of five parameters on Sh; the range of reasonable values for these five parameters yields substantial differences in Sh. Previous work on simplified bundles indicates that values for Sh are 10^{-4} – 10^{-2} (Cotton, 1998; and Cotton and Grant, 2000); accordingly, we use this range in the parametric studies reported here.

2.3. Stiffness

Since much of the literature addresses stereocilium stiffness, we calculated the non-dimensional stiffness of our model stereocilium by inverting the non-dimensional tip deflection. Redimensionalization yields stiff-

Table 3
Values of $\text{Log}_{10}(\text{Sh})$ parameter as a function of r_2/L_1 and $\text{Log}_{10}(G/kE)$

r_2/L_1	$\text{Log}_{10}(G/(kE))$				
	-1	-2	-3	-4	-5
0.10	-1.1	-0.1	0.9	1.9	2.9
0.15	-0.8	0.2	1.2	2.2	3.2
0.20	-0.5	0.5	1.5	2.5	3.5
0.25	-0.3	0.7	1.7	2.7	3.7
0.30	-0.2	0.8	1.8	2.8	3.8

ness values for the stereocilium. The linear stiffness of the stereocilium, k_x is equal to

$$k_x = \frac{F}{x} = \frac{3\pi}{4} \left(\frac{Er_2^4}{L_1^3} \right) \frac{1}{x}. \tag{10}$$

Rotational stiffness, k_θ , is the moment (M) per unit angular deflection θ (Howard and Ashmore, 1986). It is related to linear stiffness for a stereocilium of height L deflected through small angles, θ , as

$$k_\theta = \frac{M}{\theta} = \frac{FL}{\tan^{-1}(\frac{x}{L})} \cong \frac{F}{x} L^2 = k_x L^2. \tag{11}$$

2.4. Deformation profiles

Deformation profiles were examined using a computer program designed to model ciliary bundles (Cotton and Grant, 2000). This program assumes the same mechanisms described above, namely shear and bending of a cantilevered beam with a tapered base. The program uses a finite element technique to solve for deflection as a function of stereocilium height.

Several geometric combinations were examined to show deformation profiles. Model parameters are as shown in Table 1. Shaft radii were taken to be 0.18 μm . Taper height was 1.0 μm , with a minimum radii of 1/3 of the shaft radius (0.06 μm). Heights of 3, 5, 7, 10, 20, and 50 μm were simulated. Young’s modulus was $3 \times 10^9 \text{ N/m}^2$, and the shear modulus was $4 \times 10^6 \text{ N/m}^2$.

Deformation profiles were compared with profiles of a stereocilium having an infinitely stiff shaft. To do this, the cross-sectional rotation at the top of the taper was used to define the angular rotation of the shaft. Also

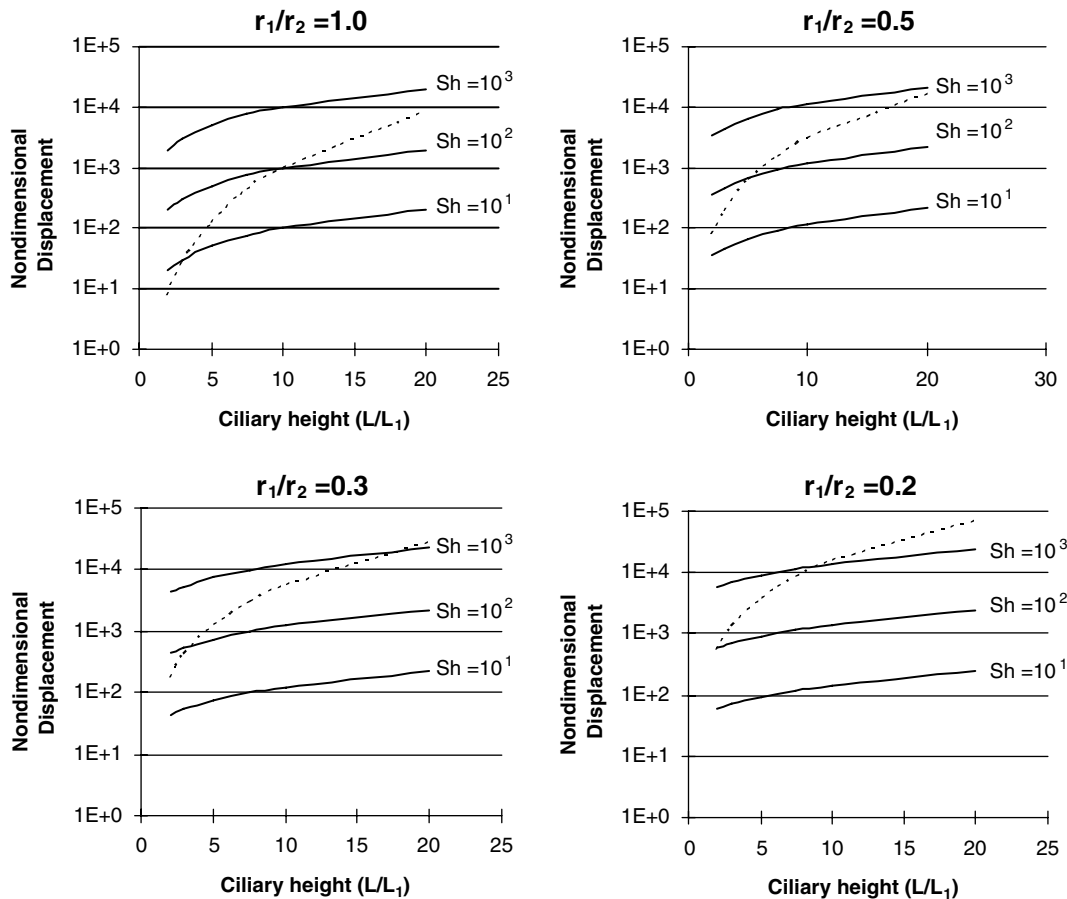


Fig. 5. Curves of single stereocilium non-dimensional deflection due to bending (dashed line) and shear (solid line) versus non-dimensional height ratio. Different degrees of non-dimensional taper are shown in the different curves. Each plot contains various values of the shear compliance Sh shown.

compared are isotropic cases where G is of the same order as E , and bending dominates.

3. Results

3.1. Tip deflection

Eqs. (5)–(7) were evaluated for different non-dimensionalized values of shear compliance Sh , taper $\bar{r}_1 = r_1/r_2$, and stereocilium height $\bar{L} = L/L_1$. Tip displacements plotted against stereocilium height (both non-dimensional) are presented in Fig. 5 for four different degrees of taper: radius ratio $\bar{r}_1 = r_1/r_2 = 1.0$ (untapered), 0.5, 0.3, and 0.2. Each plot shows the tip deflection due to bending (dashed line) and due to shear (solid lines) for shear compliances $Sh = 10^1$ – 10^3 . The shear compliance values depicted are appropriate for a transversely isotropic material where the shear modulus is several orders of magnitude less than the tensile modulus.

The contributions of bending and shear to total tip deflection increase as stereocilium height increases, but the contribution from bending increases at a higher rate than the contribution from shear. For predicted values of Sh (i.e., $Sh < 10^3$), bending dominates for tall stereocilia while shear generally dominates for the short stereocilia. Which mode dominates at any given time is strongly dependent on the value of Sh , since Sh is a linear multiplier of shear deformation (Eq. (7)). With each 10-fold increase in Sh , a 10-fold increase in tip deformation from shear is realized. The contribution from bending increases as the degree of taper increases. This is shown in more detail in Fig. 6((a) to (c)) which shows tip displacements as a function of taper (radius ratio, $\bar{r}_1 = r_1/r_2$), and for non-dimensional stereocilium heights ($\bar{L} = L/L_1$) of 3, 5, and 10. As the radius ratio $\bar{r}_1 = r_1/r_2$ increases the amount of taper decreases (when $r_1/r_2 = 1$ the stereocilium has a straight shaft with no taper). As $\bar{r}_1 = r_1/r_2$ increases, tip displacement decreases. The contribution from bending is more sensitive than that from shear; as $\bar{r}_1 = r_1/r_2$ increases tip displacement

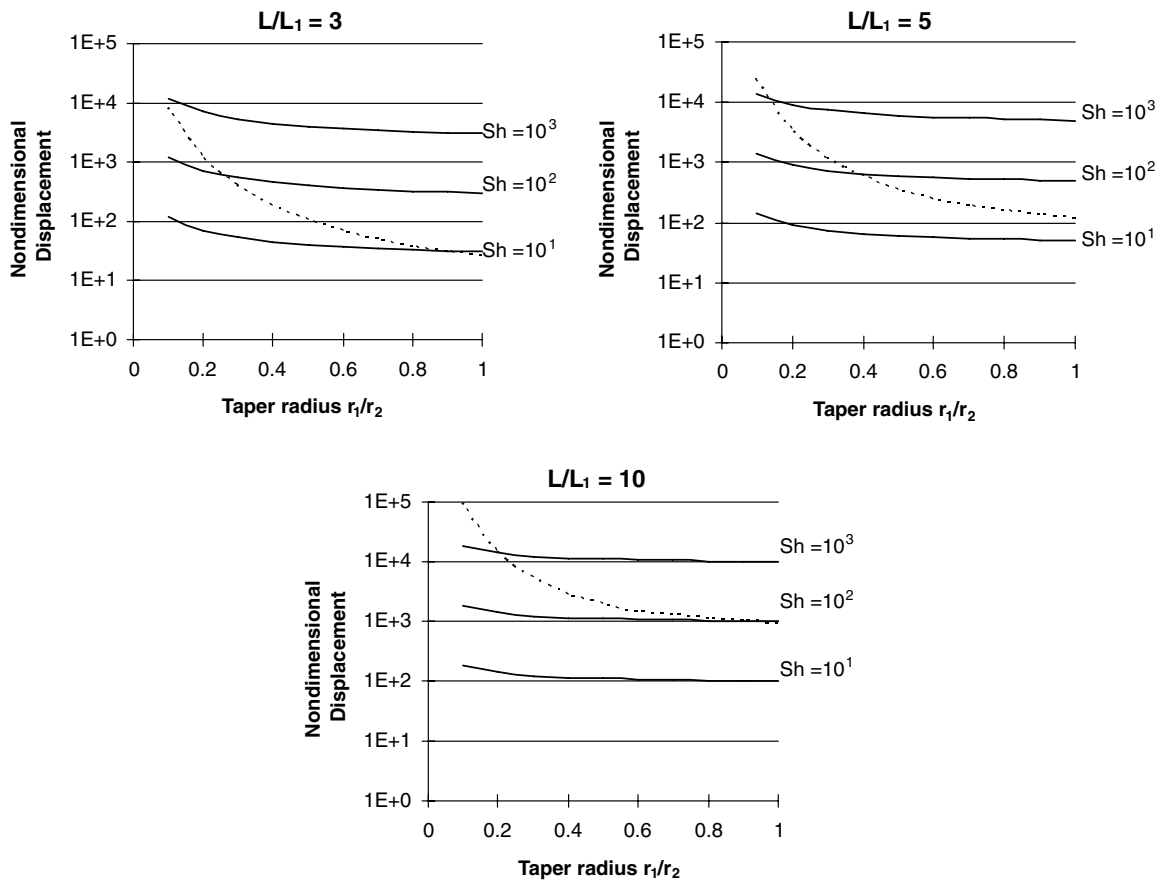


Fig. 6. Curves of single stereocilium non-dimensional deflection due to bending (dashed line) and shear (solid line) versus non-dimensional taper radius ratio. Different non-dimensional height ratios (L/L_1 =kinocilium height/taper height) are shown in the different curves. Each plot contains various values of the shear compliance Sh shown.

due to bending decreases by two orders of magnitude, while shear deformations decrease more gradually.

3.2. Stiffness

Stereocilium stiffness was redimensionalized and plotted as a function of stereocilium height in Fig. 7. As height increases, linear stiffness decreases. For the values

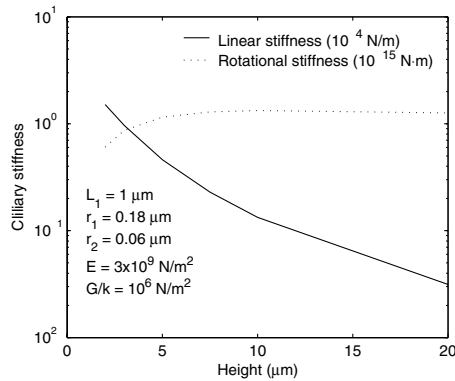


Fig. 7. Linear and rotational stiffness values of single stereocilium versus stereocilium height.

shown, height variations can cause linear stiffness variations of two orders of magnitude; the decrease in linear stiffness is even greater for stereocilia taller than 20 μm . The model gives linear stereocilium stiffness values (10^{-6} up to 10^{-4} N/m) that seem reasonable when compared to stiffness of whole hair bundles (10^{-4} – 10^{-3} , Szymko et al., 1992). Rotational stiffness is more robust to changes in height, varying from 0.6×10^{-15} to 1.3×10^{-15} N/m over the height range of 2–20 μm . These values fall within the range given by Howard and Ashmore (1986).

3.3. Deformation profiles

Fig. 8 presents predicted deformation profiles (solid line) for stereocilia of six different heights ($L=3$ – 50 μm). The predicted profiles generally resemble early qualitative descriptions of stereocilia deformations, i.e., that stereocilia bend at the base and shaft profiles are linear (Flock et al., 1977; Flock and Strekiuff, 1984). Closer examination shows that some shaft bending is visibly present in all but the shortest stereocilia. Bending of tall stereocilia is evident in published pictures of living

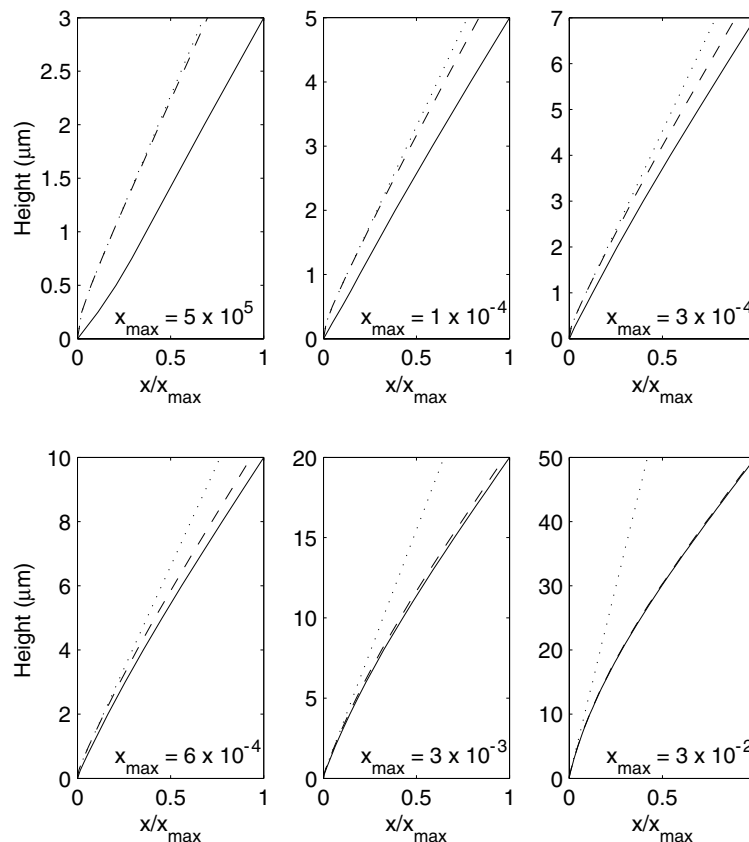


Fig. 8. Deflection profiles (solid lines) of deformed stereocilia of different heights 3, 7, 10, 20, 50 μm , based on the distributed parameter model with anisotropic material properties (shear deformation). All deflections are normalized by x_{max} , the tip deflection of that height stereocilium using the full distributed parameter model. A second deflection profile (dotted line) depicts the profile if the stereocilium were to bend only in the taper section. In this case the stereocilium is considered an infinitely stiff rod beyond its taper. The third profile (dashed line) assumes that stereocilium were isotropic, i.e. shear deformability is negligible.

hair bundles from toadfish horizontal canal (Silver et al., 1998; Fig. 4).

For comparison, Fig. 8 shows predicted deformation profiles of stereocilia modeled with more restrictive assumptions. Stereocilia with an infinitely stiff shaft (dotted line) approximate the model of Howard and Ashmore (1986). These stereocilia are stiffer, and they depart increasingly from predictions of the proposed model with increasing stereocilium height. For a 50 μm stereocilium, assumption of an infinitely stiff shaft reduces total tip deflection by 1.7 μm . Stereocilia with isotropic material properties (dashed line) undergo negligible shear deformation. Their deformation profiles approach predictions of the present model as stereocilium height increases. Thus, adoption of restrictive assumptions (no shaft bending, no shear) significantly effects the predicted deformation profile of a stereocilium, but the magnitude of the effect depends on stereocilium height.

A final observation is the noticeable shear displacement in the taper for the shortest stereocilia depicted (3 μm height). Because our proposed model does not account for known differences between the structure of the taper and the structure of the shaft (Tilney et al., 1983), this shear displacement in the taper may not occur in vivo. However the ankle links observed by Goodyear and Richardson (1994) would limit this possible shear displacement while allowing the stereocilium to bend at its base.

4. Discussion

We propose a new model for the mechanical behavior of a single stereocilium, derived from first principles of the theory of deformable bodies and experimental observations of the geometry and material properties of stereocilia. Deformable bodies theory predicts that structures with a high aspect ratio, such as a stereocilium, will bend when subjected to a point load force; thus, earlier assumptions of a perfectly rigid stereocilium shaft are unrealistic. In addition, both theory and experimental observations suggest that the stereocilium must undergo shear when deflected. The proposed model assumes that both bending and shear occur when a stereocilium is forced by a point load force at its tip.

Our model indicates that most of the bending in a stereocilium occurs at the base because the base is tapered, i.e., because the cross-sectional area is smallest at that point. The observed shear is conferred by the cross-linked f-actin fiber (transversely isotropic) composition of the stereocilium. Thus, geometric factors (base taper) and material properties (degree of transverse isotropy) must be constrained to achieve biologically realistic deformation of our model stereocilium.

Our model predicts that short stereocilia will deform as described in earlier experimental literature: they will

bend at the base and have an approximately straight shaft (Flock et al., 1977; Flock and Strekiuff, 1984). This dominate bending at the base and not much in the shaft is probably true of most cochlear bundles. Longer stereocilia, such as those in the cristae of the semicircular canals (these can reach 50–100 μm height), will exhibit significant bending of the shaft. Such bending of stereocilia has been observed experimentally in an entire bundle (Silver et al., 1998). Parametric analyses suggest that total tip deflection and the relative contributions of bending and shear to total tip deflection will depend on three factors: (1) the shear compliance of the stereocilium material, (2) the degree of base taper, and (3) stereocilium height.

The use of finite element methods has allowed us to predict the deformation profile of a stereocilium when it is forced by a point load at its tip. If the goal is simply to determine total tip deflection, then profile shape is not important. However, if the stereocilium model is incorporated into a model of a (partial or complete) hair bundle, it must not only describe tip deflection accurately, but also the deflection at all points of link attachment along the length of the stereocilium. This is true because the lateral links that connect stereocilia are relatively stiff compared to the stereocilia (Pickles, 1993; Cotton, 1998). Thus, small errors in predicting deformation profiles will be transmitted faithfully between stereocilia, and the in-series arrangement of stereocilia in a bundle will magnify these small errors as deflection cascades down the excitatory/inhibitory axis of the bundle.

Acknowledgements

This work was supported by the National Institute of Health R01 DC05063, and the National Science Foundation IBN-9724123.

References

- Beer, F.P., Johnston, E.R., 2001. *Mechanics of Materials*, third ed. McGraw Hill, New York.
- Boresi, A.P., Schmidt, R.J., Sidebottom, O.M., 1993. *Advanced Mechanics of Materials*, fifth ed. John Wiley and Sons, New York, p. 178.
- Cotton, J.R., 1998. *Mechanical Models of Vestibular Hair Cell Bundles*. Ph.D. Dissertation, Virginia Polytechnic Institute and State University, Blacksburg, VA.
- Cotton, J., Grant, J.W., 2000. A finite element method for mechanical response of hair cell ciliary bundles. *Journal of Biomechanical Engineering* 122, 44–50.
- Duncan, R.K., 1993. *Finite Element Analysis of Inner Ear Hair Bundles: A Parameter Study of Bundle Mechanics*. Thesis, Virginia Polytechnic Institute and State University, Blacksburg, VA.
- Duncan, R.K., Eisen, M.D., Saunders, J.C., 1999. Distal separation of chick cochlear hair cell stereocilia: analysis of constant-constraint models. *Hearing Research* 127, 22–30.
- Duncan, R.K., Grant, J.W., 1998. A finite element model of inner ear hair bundle micromechanics. *Hearing Research* 104, 15–26.

- Flock, A., Cheung, H.C., 1974. Actin filaments in sensory hairs of inner ear receptor cells. *Journal of Cell Biology* 75, 339–343.
- Flock, A., Strelhoff, C., 1984. Graded and nonlinear properties of sensory hairs in the mammalian hearing organ. *Nature* 310, 597–599.
- Flock, A., Flock, B., Murray, E., 1977. Studies on the sensory hairs of receptor cells in the inner ear. *Acta Otolaryngologica* 83, 85–91.
- Gittes, F., Mickey, B., Nettleton, J., Howard, J., 1993. Flexural rigidity of microtubules and actin filaments measured from thermal fluctuation in shape. *Journal of Cell Biology* 120, 923–924.
- Goodyear, R., Richardson, G., 1994. Differential glycosylation of auditory and vestibular hair bundle proteins revealed by peanut agglutinin. *Journal of Comparative Neurology* 345, 267–278.
- Howard, J., Ashmore, J.F., 1986. Stiffness of sensory hair bundles in the sacculus of the frog. *Hearing Research* 23, 93–104.
- Howard, J., Roberts, W.M., Hudspeth, A.J., 1988. Mechano-electrical transduction by hair cells. *Annual Review of Biophysics and Biophysical Chemistry* 17, 99–124.
- Jones, R.M., 1999. *Mechanics of Composite Materials*, second ed. McGraw-Hill, New York.
- Lewis, E.R., Leverenz, E.L., Bialek, W.S., 1985. *The Vertebrate Ear*. CRC Press, Boca Raton, FL.
- Lim, D.J., 1977. Ultra anatomy of sensory end-organs in the labyrinth and their functional implications. In: Shambaugh, G.E. Jr, Shea, J.J., (Eds.), *Proceedings of the Shambaugh Fifth International Workshop on Middle Ear Microsurgery and Fluctuant Hearing Loss*, pp. 16–27.
- Lindeman, H.H., 1973. Anatomy of the otolith organs. *Advances in Otorhinolaryngology* 20, 405–433.
- Pickles, J.O., 1993. A model for the mechanics of the stereociliar bundle on acousticolateral hair cells. *Hearing Research* 68, 159–172.
- Pickles, J.O., Corey, D.P., 1992. Mechano-electrical transduction by hair cells. *Trends in Neurosciences* 15, 254–258.
- Saunders, J.C., Schneider, M.E., Dear, S.P., 1985. The structure and function of actin in hair cells. *Journal of the Acoustic Society of America* 78 (1 Pt 2), 299–311.
- Silver, R.B., Reeves, A.P., Steinacker, A., Highstein, S.M., 1998. Examination of the cupula and stereocilia of the horizontal semicircular canal in the toadfish *Opsanus tau*. *Journal of the Comparative Neurology* 402, 48–61.
- Szymko, Y., Dimitri, P., Saunders, J., 1992. Stiffness of hair bundles in chick cochlea. *Hearing Research* 59, 241–249.
- Tilney, L.G., Egelman, E.H., DeRosier, D.J., Saunders, J.C., 1983. Actin filaments, stereocilia, and hair cells of the bird cochlea. II. Packing of the actin filaments in the stereocilia and in the cuticular plate and what happens to the organizations when the stereocilia are bent. *Journal of Cell Biology* 96, 822–834.